

Interference With Peroxisome Proliferator-Activated Receptor- γ in Vascular Smooth Muscle Causes Baroreflex Impairment and Autonomic Dysfunction

Giulianna R. Borges, Donald A. Morgan, Pimonrat Ketsawatsomkron, Aaron D. Mickle, Anthony P. Thompson, Martin D. Cassell, Durga P. Mohapatra, Kamal Rahmouni, Curt D. Sigmund

Abstract—S-P467L mice expressing dominant negative peroxisome proliferator-activated receptor- γ selectively in vascular smooth muscle exhibit impaired vasodilation, augmented vasoconstriction, hypertension, and tachycardia. We hypothesized that tachycardia in S-P467L mice is a result of baroreflex dysfunction. S-P467L mice displayed increased sympathetic traffic to the heart and decreased baroreflex gain and effectiveness. Carotid arteries exhibited inward remodeling but no changes in distensibility or stress/strain. Aortic depressor nerve activity in response to increased arterial pressure was blunted in S-P467L mice. However, the arterial pressure and heart rate responses to aortic depressor nerve stimulation were unaltered in S-P467L mice, suggesting that the central and efferent limbs of the baroreflex arc remain intact. There was no transgene expression in nodose ganglion and no change in expression of the acid-sensing ion channel-2 or -3 in nodose ganglion. There was a trend toward decreased expression of transient receptor potential vanilloid-1 receptor mRNA in nodose ganglion, but no difference in the immunochemical staining of transient receptor potential vanilloid-1 receptor in the termination area of the left aortic depressor nerve in S-P467L mice. Although there was no difference in the maximal calcium response to capsaicin in cultured nodose neurons from S-P467L mice, there was decreased desensitization of transient receptor potential vanilloid-1 receptor channels. In conclusion, S-P467L mice exhibit baroreflex dysfunction because of a defect in the afferent limb of the baroreflex arc caused by impaired vascular function, altered vascular structure, or compromised neurovascular coupling. These findings implicate vascular smooth muscle peroxisome proliferator activated receptor- γ as a critical determinant of neurovascular signaling. (*Hypertension*. 2014;64:590-596.) • [Online Data Supplement](#)

Key Words: baroreflex ■ blood pressure ■ heart rate ■ muscle, smooth, vascular ■ peroxisome proliferator-activated receptors ■ sympathetic nervous system

Peroxisome proliferator-activated receptor- γ (PPAR γ) is a ligand-activated transcription factor belonging to the nuclear receptor superfamily. Classically, PPAR γ plays an important role in adipogenesis and metabolic processes but has recently emerged as a crucial element in cardiovascular diseases such as hypertension. Mutations of PPAR γ lead to hypertension in humans and in experimental animal models.^{1,2} Moreover, thiazolidinediones, high-affinity PPAR γ agonists, which increase insulin sensitivity, have been shown to be helpful in lowering arterial pressure (AP) and improving vascular function.³

We have previously shown that mice carrying a dominant-negative form of PPAR γ specifically in smooth muscle (S-P467L mice) exhibit hypertension, severe aortic dysfunction, and hypertrophy of cerebral arterioles.⁴ Vascular

dysfunction occurs because of impaired expression of the PPAR γ target gene regulator of G-protein signaling 5 (*RGS5*) leading to enhanced myogenic tone and angiotensin-II-mediated contraction in the mesenteric circulation, and impaired function of the cullin-3, cullin ring ligase pathway leading to increased RhoA and Rho kinase activity in the aorta.^{5,6} Interestingly, these transgenic mice also exhibited robust tachycardia despite increased systemic AP, suggesting that interference with vascular smooth muscle PPAR γ may impair the baroreflex.⁴

The baroreflex is an important beat-to-beat regulator of AP and heart rate (HR). Baroreceptors, located in the adventitia of the aortic arch and carotid sinus, provide a highly sensitive system that detects changes in AP. These receptors send afferent signals to the central nervous system, and the efferent

Received March 14, 2014; first decision April 2, 2014; revision accepted May 14, 2014.

From the Department of Pharmacology (G.R.B., D.A.M., P.K., A.D.M., D.P.M., K.R., C.D.S.), Department of Anatomy and Cell Biology (A.P.T., M.D.C.), and Center on the Functional Genomics of Hypertension (K.R., C.D.S.), Roy J. and Lucille A. Carver College of Medicine, University of Iowa, Iowa City.

The online-only Data Supplement is available with this article at <http://hyper.ahajournals.org/lookup/suppl/doi:10.1161/HYPERTENSIONAHA.114.03553/-/DC1>.

Correspondence to Curt D. Sigmund, Department of Pharmacology, Roy J. and Lucille A. Carver College of Medicine, University of Iowa, 375 Newton Rd, 3181 MERF, Iowa City, Iowa 52242. E-mail curt-sigmund@uiowa.edu

© 2014 American Heart Association, Inc.

Hypertension is available at <http://hyper.ahajournals.org>

DOI: 10.1161/HYPERTENSIONAHA.114.03553

innervation of blood vessels, heart, and kidneys make adjustments to maintain normal AP.⁷ Clinical and experimental hypertension commonly involves cardiovascular autonomic impairment associated with high sympathetic activity and blunted baroreflex sensitivity with baroreceptor resetting.⁸ In this study, we hypothesize that the tachycardia observed in S-P467L mice is attributable to cardiovascular autonomic impairment and baroreflex dysfunction. Our data suggest that impairment in PPAR γ function in smooth muscle can impair neurovascular coupling, which can attenuate afferent signaling to the central nervous system.

Materials and Methods

A detailed description of the transgenic mouse model, baseline cardiovascular measures, assessment of baroreflex sensitivity and efficacy, spectral analysis, mechanical properties of carotid artery, primary cultures of mouse nodose ganglia (NG), neurovascular coupling including calcium imaging as a measure of transient receptor potential vanilloid-1 receptor channels (Trpv1) functional properties, molecular measures, and data and statistical analysis are provided in the online-only Data Supplement. All studies were approved by the Institutional Animal Care and Use Committee in compliance with the National Institutes of Health Guide for the Care and Use of Laboratory Animals.

Results

We first measured AP and HR with radiotelemetry. S-P467L mice exhibited elevated AP (Figure 1A) and were markedly tachycardic (Figure 1B). Intrinsic HR, measured after simultaneous sympathetic and parasympathetic blockade, was elevated in S-P467L mice (Figure 1B). Consistent with increased sympathetic outflow to the heart, we observed a larger bradycardic response in S-P467L mice after administering the β -adrenergic antagonist propranolol (Figure 1C). Similarly, the methyl-atropine induced tachycardic response was significantly smaller in S-P467L mice. Power spectral analysis revealed comparable relative low-frequency and high-frequency components between groups (Figure S1A in the online-only Data Supplement). The low-frequency component of HR (Figure S1B) and AP (Figure S1C) predominated in S-P467L mice. S-P467L mice also exhibited increased systolic AP variability (Figure S1D). Applying the sequence method to examine spontaneous baroreflex fluctuations of AP revealed no changes in the number of sequences (Figure S1E), but S-P467L mice exhibited decreases in both baroreflex gain (Figure S1F) and effectiveness (Figure S1G).

To assess whether the impairment in baroreflex function is because of alterations in vessel structure or function or both,

the mechanical properties of carotid arteries were determined in the absence of vascular tone. The lumen diameter was significantly reduced in S-P467L carotid arteries across all pressures tested (Figure 2A). However, there were no differences in vascular distensibility (Figure 2B), and although the stress-strain curve was shifted to the right in S-P467L carotid arteries, the slope was not statistically different between the groups (Figure 2C, nontransgenic: 2.61 ± 0.03 , S-P467L: 2.38 ± 0.11 ; $P > 0.05$), suggesting a similar stiffness.

Because baroreflex dysfunction in S-P467L mice could originate from either the afferent or the central (efferent) limb, we analyzed AP and HR in conjunction with aortic depressor nerve (ADN) activity at baseline and in response to various stimuli. We first examined the HR response to phenylephrine and sodium nitroprusside in nontransgenic and S-P467L mice under conscious conditions. S-P467L mice exhibited tachycardia at baseline (621 ± 18 versus 527 ± 26 bpm; $P < 0.01$) and moderately elevated systolic AP (149.3 ± 10.1 versus 139.5 ± 8.4 mmHg). S-P467L and nontransgenic mice exhibited equivalent pressor and depressor responses to phenylephrine and sodium nitroprusside, respectively (Figure 3A). Although both S-P467L and nontransgenic mice exhibited similar tachycardic responses to sodium nitroprusside, the bradycardic response to phenylephrine was significantly blunted in S-P467L mice (Figure 3B).

We next measured ADN activity in nontransgenic and S-P467L mice under anesthesia. ADN activity occurred in bursts and was synchronous with the AP pulse in both nontransgenic and S-P467L mice (Figure S2; Figure 4A and 4B).⁹ There was no difference in baseline ADN activity between S-P467L (95 ± 13 spikes/s) and nontransgenic (97 ± 9 spikes/s) mice. The ADN response to sodium nitroprusside was comparable between nontransgenic and S-P467L mice (Figure 4C and 4D). ADN activity rose abruptly in response to the pressor effects of phenylephrine in both groups, but the magnitude of the response was markedly blunted in S-P467L mice (Figure 4C and 4D).

The sigmoidal fitting ADN-AP curve is shown in Figure 5. The baroreflex range, gain, and saturation pressure (MAPsat) were all significantly decreased in S-P467L mice, whereas the mean arterial pressure at 50% of ADN activity and threshold pressure were not different between groups (Table). To examine the central integration of the afferent signal, we directly stimulated the ADN and monitored changes in AP and HR. Unlike the impaired response in S-P467L induced by acute

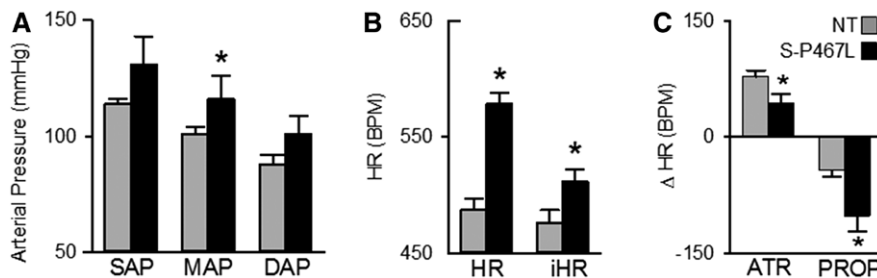


Figure 1. Arterial pressure and heart rate. Measurement of systolic arterial pressure (SAP), mean arterial pressure (MAP), diastolic arterial pressure (DAP), heart rate (HR), and intrinsic heart rate (iHR), using radiotelemetry. **A**, Average 1-hour recording of SAP, MAP, and DAP. **B**, Average HR over a 1-hour period calculated from the arterial pressure (AP) recordings and iHR calculated from the AP recordings after simultaneous blockage of sympathetic and vagal tone to the heart with propranolol and methyl-atropine, respectively. **C**, HR response to intraperitoneal injection of methyl-atropine (ATR) and propranolol (PROP). S-P467L (black) and nontransgenic (gray) mice. * $P < 0.05$ vs nontransgenic (NT; $n = 8$).

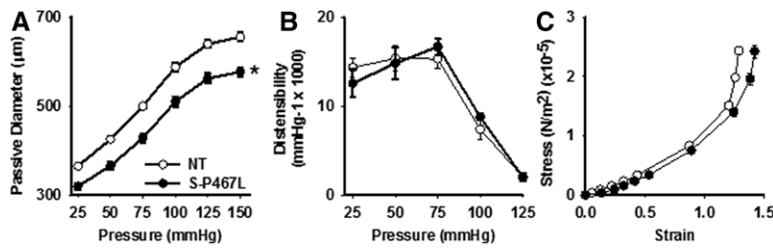


Figure 2. Vascular mechanics. **A**, The passive diameter of the carotid artery was assessed under calcium-free conditions in response to increases in intraluminal pressure. **B**, Distensibility was calculated from the pressure diameter relationship. S-P467L (n=6); nontransgenic (NT; n=5); * $P < 0.05$ vs NT. **C**, A stress-strain curve was calculated from the internal and external diameter of the vessels that were exposed to a series of pressure steps from 0, 10, 20, 30, 50, 75, 100, 125 to 150 mmHg. S-P467L (n=4); NT (n=3).

increase in AP, the systolic AP and HR responses to ADN stimulation exhibited no differences between groups (Figure 6).

We next determined whether defects in the NG contribute to the impaired baroreflex sensitivity in S-P467L mice. Because PPAR γ expression was recently identified in nodose neurons, we first assessed whether the smooth muscle promoter-driven transgene was expressed in NG in S-P467L mice.¹⁰ No signal was detected in either the aorta or NG of nontransgenic mice. Although a signal (Ct value ≈ 28) was detected in NG from S-P467L mice, it was expressed ≈ 500 -fold less than in the aorta (Figure S3A). There was no significant change in expression of the PPAR γ target genes CD36 or aP2 in NG from P467L compared with nontransgenic (data not shown). Previous studies reported that the acid-sensing ion channel-2 (ASIC2) is expressed in aortic baroreceptor neurons and that *Asic2*-deficient mice exhibit baroreflex dysfunction.¹¹ However, there was no difference in the level of expression of either *Asic2* (Figure S3B) or *Asic3* (Figure S3C) mRNA in the NG of S-P467L mice. Trpv1 receptor channels have been implicated in baroreflex function,¹² but there was no detectable expression of Trpv1 mRNA in the aorta. Initial investigations suggested a decrease in mRNA encoding Trpv1 in NG from S-P467L mice, but ultimately, this trend was not significant (Figure S3D). Based on our early finding, we assessed whether there was histological evidence to support a defect in neural vascular coupling at the aorta arch. No obvious differences were observed between nontransgenic and S-P467L mice in the immunohistochemical staining pattern of Trpv1 in the termination area of the left ADN (Figure 7A–7F). In all specimens, both thick and thin fibers could be seen arising from the ADN in the aortic wall and bouton-like swellings and heavily branched terminal arrays similar to those reported elsewhere.¹³ The mean numbers of grid intersections were 18.9 ± 15.5 and

18.6 ± 10.7 (nontransgenic versus S-P467L, $t = 0.237$; $P = 1.0$) for large fibers and 6.57 ± 7.9 and 9.2 ± 7.81 (nontransgenic versus S-P467L, $t = 0.851$; $P = 0.4$), indicating that there was no difference between the mean number of large fiber intersections and only a modest difference for fine fiber intersections.

Finally, we examined whether there was any change in the number of functional Trpv1 channels in the NG neurons by monitoring Trpv1-mediated increase in intracellular Ca^{2+} ($[Ca^{2+}]_i$) responses (Figure 7G).¹⁴ No significant change was observed in the magnitude of capsaicin-induced $[Ca^{2+}]_i$ rise, normalized to the KCl-induced $[Ca^{2+}]_i$ rise in NG neurons of either genotype (Figure 7H), indicating no change in the levels of functional Trpv1 channel in these neurons. Interestingly, there was a significant decrease in the magnitude of Trpv1 channel desensitization in the NG neurons from S-P467L mice (Figure 7I).

Discussion

There is emerging evidence that the ligand-activated transcription factor PPAR γ , best known for its regulation of adipogenesis, lipid metabolism, and insulin sensitivity, plays autocrine roles in tissues outside of its classical sites of action (eg, liver, skeletal muscle, and adipose tissue). Endothelial PPAR γ -deficiency (through gene ablation) or PPAR γ -interference (using a dominant-negative mutant) results in impaired nitric oxide-mediated vasodilatation and increased AP in response to a high-fat diet.^{15–17} Smooth muscle PPAR γ -deficiency blunts the protective effects of thiazolidinediones on atherosclerosis and augments angiotensin II-induced oxidative stress, inflammation, and vascular remodeling.^{18,19} Selective vascular smooth muscle interference with PPAR γ causes a loss of nitric oxide responsiveness, an increase in vasoconstriction, and hypertension.⁴

Despite mild hypertension, S-P467L mice exhibit robust tachycardia, suggesting impaired autonomic function.⁴ S-P467L mice exhibited a blunted tachycardic response to vagal blockade and a markedly augmented bradycardic response to sympathetic blockade. The direct measurements of HR in response to pharmacological blockade suggest that there is increased sympathetic activity to the heart. This conclusion was further supported by spectral analysis, although it should be noted that the application and usefulness of spectral analysis remains controversial.

HR can be controlled by baroreceptors and chemoreceptors on free nerve endings in the aortic arch and carotid sinus, which transmit afferent signals to the brain in response to the local stretch of the vessel or changes in oxygen or pH.^{20,21} Theoretically, a lesion in any portion of the baroreflex arc can lead to baroreflex impairment. That the ADN response to an increase in AP was severely impaired in S-P467L mice

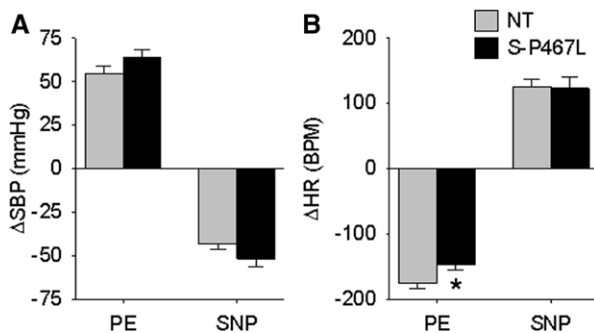


Figure 3. Blood pressure (BP) and heart rate (HR) response to phenylephrine (PE) and sodium nitroprusside (SNP). The change in systolic BP (SBP; **A**) and HR (**B**) in conscious S-P467L and nontransgenic (NT) mice is shown in response to slow intravenous infusion of PE (5 μ g) followed by SNP (5 μ g).

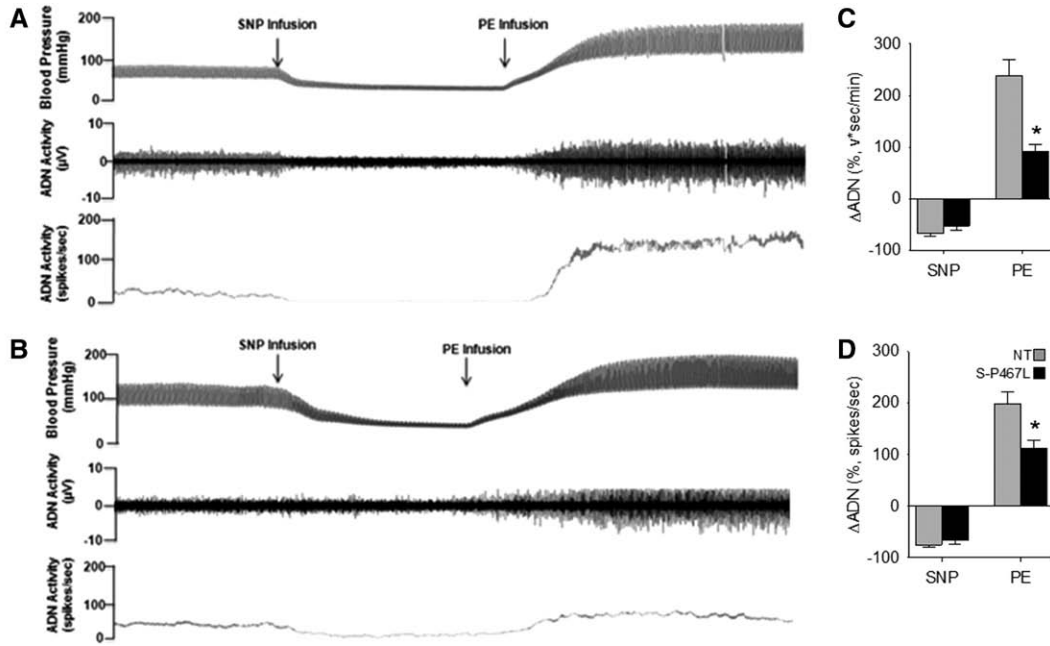


Figure 4. Relationship between arterial pressure, heart rate, and aortic depressor nerve activity. Representative tracings of blood pressure and aortic depressor nerve (ADN) activity in anesthetized nontransgenic (NT; **A**) and S-P467L (**B**) mice. The change in ADN activity (**C** and **D**) is shown in response to changes in arterial pressure induced by infusion of sodium nitroprusside (SNP) followed by phenylephrine (PE). S-P467L (black) and nontransgenic (gray) mice. NT (n=10); S-P467L (n=8); **P*<0.05 vs NT.

suggests impairment in the afferent limb of the baroreflex arc. That the HR response to direct ADN stimulation was normal suggests that the central and efferent limbs of the baroreflex are functioning normally. This stands in contrast to other models of hypertension including the spontaneously hypertensive rat, deoxycorticosterone acetate-salt-treated rat, and obese Zucker rat, where the depressor response elicited by direct stimulation of ADN was attenuated suggesting a defect in the central component of the baroreflex arc.²²⁻²⁴ Unlike the spontaneously hypertensive rat, which exhibits marked hypertension, the S-P467L mouse model displays only a small increase in arterial blood pressure but profound baroreflex dysfunction. Therefore, it is unlikely that the baroreflex dysfunction observed in S-P467L mice is because of increased AP.

The mechanical properties of the vascular wall and substances released by vascular cells have major influence on baroreceptor activity. For example, impaired release of

prostacyclin, increased generation of reactive oxygen species, and platelet aggregation have been shown to reduce baroreceptor activity during hypertension and atherosclerosis.²⁵ Apolipoprotein E-deficient mice were reported to exhibit both hypertension and tachycardia, suggesting that hypercholesterolemia, atherosclerosis, or vascular structure and function or all of these may affect baroreflex regulation.²⁶ Vascular hypertrophy has been previously associated with the degree of baroreflex impairment.²⁷ We showed here that there was a decrease in the diameter (without a change in wall thickness) of the carotid artery, and our previous observations indicate that cerebral arterioles, but not mesenteric arteries, in S-P467L mice undergo hypertrophy, increased distensibility, and remodeling.^{4,5} Thus, we must consider the possibility that the baroreceptor afferents in S-P467L mice may be unresponsive to increases in AP because of structural changes in the vessel. Alternatively, functional defects in the vessel may be playing an important role. Previous ex vivo studies revealed that the aorta from S-P467L mice exhibits markedly impaired responses to both endogenous

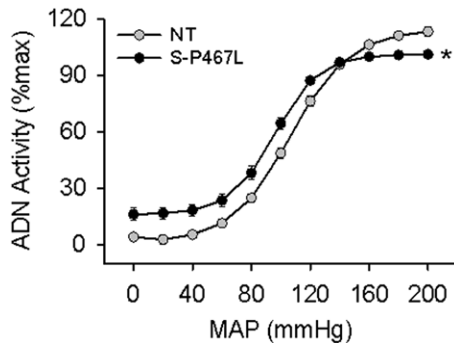


Figure 5. Baroreflex curves. Analysis of baroreceptor afferent function curves derived from responses to intravenous injections of sodium nitroprusside and phenylephrine in S-P467L (filled circles) and nontransgenic (NT; open circles) mice. ADN indicates aortic depressor nerve; and MAP, mean arterial pressure.

Table. Baroreflex Parameters

Parameter	NT	S-P467L
Range, mm Hg	114±4	85±4*
Gain, %max	1.69±0.08	1.26±0.05*
MAP50, mm Hg	101±2.4	95±2
MAPth, mm Hg	45±2	46±4.9
MAPsat, mm Hg	172±5.3	156±3.8*

Tabulated data derived from individual curves. NT (n=10); S-P467L (n=8). MAP50 indicates mean arterial pressure at 50% of aortic depressor nerve activity; MAPsat, mean arterial saturation pressure; MAPth, mean arterial threshold pressure; and NT, nontransgenic.

**P*<0.05 vs NT.

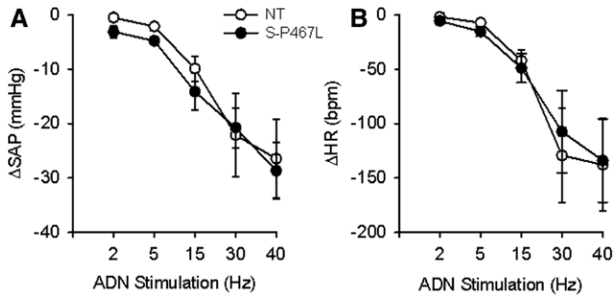


Figure 6. Heart rate (HR) and arterial pressure (AP) responses to aortic depressor nerve (ADN) stimulation. Reflex decreases in systolic AP (Δ SAP, **A**) and heart rate (Δ HR, **B**) in response to electric stimulation of the ADN in anesthetized S-P467L (filled circles) and nontransgenic (NT; open circles) mice ($n=9$ per group).

and exogenous nitric oxide.^{4,6,28} Interestingly, mesenteric vessels from S-P467L mice display large conductance Ca^{2+} -activated K^+ channel dysfunction,⁵ and polymorphisms in the *KCNMB1* gene encoding the $\beta 1$ subunit is associated with HR variability and baroreflex function in humans.²⁹

PPAR γ is expressed in primary cultured microglia and cortical neurons where its protective effects may be a result of its antioxidant and anti-inflammatory actions.^{30,31} PPAR γ is also expressed in the arcuate nucleus of the hypothalamus where it regulates the activity of a subset of neurons to control food intake.^{32,33} Nevertheless, it remains unclear whether PPAR γ is expressed in the afferent nerves communicating baroreflex signals from the peripheral vasculature to the brain. Recently, PPAR γ expression in the vagal nerve was reported to play a role in high-fat diet-induced thermogenesis.¹⁰ We found no evidence for the expression of the transgene encoding dominant-negative PPAR γ , nor a change in expression of 2 PPAR γ target genes in peripheral NG nerves. Thus, PPAR γ in nerves derived from the aortic arch and carotid sinus baroreceptors was unlikely to be affected. *Asic2*, *Asic3*, and *Trpv1* have been mechanistically implicated to modulate the baroreflex.^{11,12} There was no change in *Asic* channel expression, but initial studies suggested that expression of *Trpv1* might be decreased. This was attractive because *Trpv1* channels are localized on the nerve fibers and terminals in the aortic arch and in NG neurons and because ablation or inhibition of *Trpv1*-containing neurons blunts the baroreflex.¹² Although there were no detectable

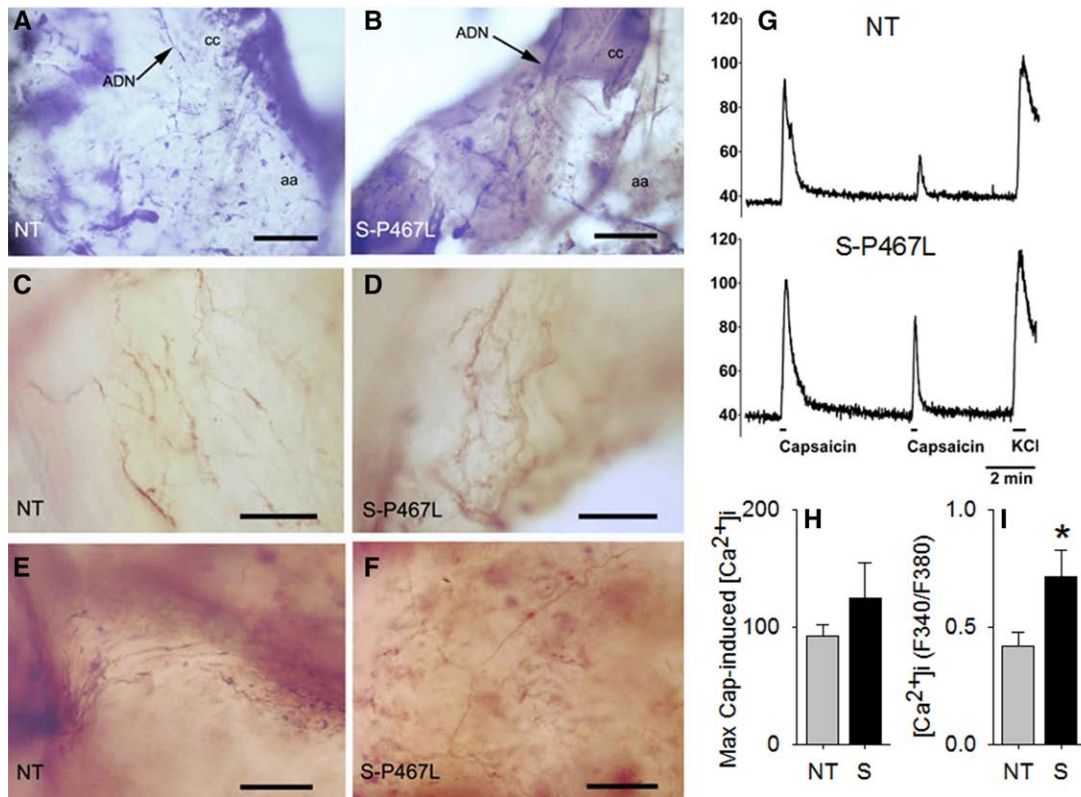


Figure 7. Neurovascular coupling and function of transient receptor potential vanilloid 1 receptor (*Trpv1*) channels in nodose ganglia neurons. Fibers and terminals of the aortic depressor nerve (ADN) on the aortic arch (aa) immunochemically stained with an antibody against *Trpv1* in nontransgenic (NT) and S-P467 transgenic mice. **A**, Low-power micrograph from a whole-mount preparation from a NT animal showing the ADN innervating the region of the aortic arch at the junction with the left common carotid artery (cc). **B**, Preparation similar to that in **A** from a S-P467L mouse. Note the similar appearance of the ADN and its arborizations in both mice. **C** and **D**, Complex endings of *Trpv1* positive ADN axons in the vicinity of the aortic arch-left carotid junction. **E** and **F**, Arborizations of thin *Trpv1* positive axons on the anterior wall of the aortic arch. Scale bars in **A** and **B**, 250 μ m; scale bars in **C–F**, 25 μ m. **G**, Representative traces of Ca^{2+} imaging in response to 2 successive capsaicin applications (100 nmol/L, 15 seconds), followed by KCl application (50 mmol/L, 30 seconds) in nodose ganglia neurons. **H**, Maximal capsaicin-induced intracellular Ca^{2+} ($[Ca^{2+}]_i$) responses normalized to KCl. **I**, Magnitude of *Trpv1* desensitization, expressed as the ratio of second vs first capsaicin-induced peak $[Ca^{2+}]_i$ in the same neuron. $n=38$ for NT and $n=58$ for S-P467L (* $P<0.05$ vs NT).

differences in the number of Trpv1-expressing fibers at the termination of the left ADN, and no change in the maximal response to the Trpv1 ligand capsaicin, there was a significant decrease in the extent of channel desensitization in cultured NG neurons from S-P467L mice. This decrease in the magnitude of Trpv1 desensitization could lead to prolonged channel opening duration, which could promote action potential firing, that is, increased excitation of these neurons on Trpv1 activation. Physiologically, the Trpv1 channel could be activated by acidic pH (≤ 6.0) or noxious temperatures ($\geq 43^\circ\text{C}$).³⁴ However, pathological conditions (eg, inflammation) could lead to the activation of Trpv1 at normal body temperature, as well as by relatively weak acidic pH (≈ 6.8 – 6.4).^{14,35} Under such circumstances, if the Trpv1 channel desensitization is decreased, it could lead to prolonged excitation of NG neurons. Of course, we recognize that this would stand in apparent contradiction to data showing that loss of Trpv1 causes baroreceptor dysfunction.¹² It is also possible that the decrease in channel desensitization constitutes a compensatory effect elicited by the decrease in Trpv1 expression, which could ultimately lead to a normalization of channel function.

Perspectives

The most important observations from this study are that mice with impaired PPAR γ activity in vascular smooth muscle exhibit tachycardia mechanistically caused by any combination of the following: (1) increased cardiac sympathetic nervous system activity, (2) impaired baroreflex, and (3) a blunted ADN response to increased AP localized to the afferent limb of the baroreflex arc. Therefore, there may be some degree of baroreflex failure in S-P467L mice, which drives the increased HR.

Alteration in baroreflex function is a common problem in diabetes mellitus. Baroreflex sensitivity is decreased in patients with impaired glucose tolerance³⁶ and is blunted in patients with diabetes mellitus.³⁷ Likewise, animal models of diabetes mellitus display baroreflex alterations in a similar fashion to human diabetes mellitus.^{38,39} Depressed baroreflex sensitivity was reported to be predictive of other cardiovascular events in diabetes mellitus.⁴⁰ Of greatest relevance to the current study, pioglitazone, a high-affinity synthetic PPAR γ agonist, increased baroreflex sensitivity in type II patients with diabetes mellitus.⁴¹ Similarly, rosiglitazone, another member of the thiazolidinedione family of PPAR γ agonists, improves baroreflex gain in rats with diet-induced obesity.⁴² Given that diabetes mellitus is often associated with PPAR γ impairment, these findings combined with our current study raise the possibility that diabetes mellitus-associated baroreflex alteration is a result of defective vascular PPAR γ . Indeed our findings implicate vascular smooth muscle PPAR γ as a critical determinant of neurovascular signaling. Thus, S-P467L mice may be a useful model to understand the decreased baroreflex sensitivity in diabetes mellitus.

Acknowledgments

We thank Deborah R. Davis for assistance with mice. We also thank Norma Sinclair, JoAnne Schwarting, and Patricia Yarolem for genotyping mice. Transgenic mice were generated at the University of Iowa Transgenic Animal Facility supported in part by grants from the National Institutes of Health and from the Roy J. and Lucille A. Carver College of Medicine.

Sources of Funding

This work was supported through research grants from the National Institutes of Health to C.D. Sigmund and K. Rahmouni (HL084207), to C.D. Sigmund (HL048058, HL061446, and HL062984), to A.D. Mickle (CA171927), and to D.P. Mohapatra (NS069898) and from the American Heart Association to P. Ketsawatsomkron (11POST5720021) and K. Rahmouni (14EIA18860041). We also gratefully acknowledge the generous research support of the Roy J. Carver Trust.

Disclosures

None.

References

- Barroso I, Gurnell M, Crowley VE, Agostini M, Schwabe JW, Soos MA, Maslen GL, Williams TD, Lewis H, Schafer AJ, Chatterjee VK, O'Rahilly S. Dominant negative mutations in human PPAR γ associated with severe insulin resistance, diabetes mellitus and hypertension. *Nature*. 1999;402:880–883.
- Beyer AM, Baumbach GL, Halabi CM, Modrick ML, Lynch CM, Gerhold TD, Ghoneim SM, de Lange WJ, Keen HL, Tsai YS, Maeda N, Sigmund CD, Faraci FM. Interference with PPAR γ signaling causes cerebral vascular dysfunction, hypertrophy, and remodeling. *Hypertension*. 2008;51:867–871.
- Ryan MJ, Didion SP, Mathur S, Faraci FM, Sigmund CD. PPAR(γ) agonist rosiglitazone improves vascular function and lowers blood pressure in hypertensive transgenic mice. *Hypertension*. 2004;43:661–666.
- Halabi CM, Beyer AM, de Lange WJ, Keen HL, Baumbach GL, Faraci FM, Sigmund CD. Interference with PPAR γ function in smooth muscle causes vascular dysfunction and hypertension. *Cell Metab*. 2008;7:215–226.
- Ketsawatsomkron P, Lorca RA, Keen HL, Weatherford ET, Liu X, Pelham CJ, Grobe JL, Faraci FM, England SK, Sigmund CD. PPAR γ regulates resistance vessel tone through a mechanism involving RGS5-mediated control of PKC and BKCa channel activity. *Circ Res*. 2012;111:1446–1458.
- Pelham CJ, Ketsawatsomkron P, Groh S, Grobe JL, de Lange WJ, Ibeawuchi SR, Keen HL, Weatherford ET, Faraci FM, Sigmund CD. Cullin-3 regulates vascular smooth muscle function and arterial blood pressure via PPAR γ and RhoA/Rho-kinase. *Cell Metab*. 2012;16:462–472.
- Dampney RA. Functional organization of central pathways regulating the cardiovascular system. *Physiol Rev*. 1994;74:323–364.
- Parati G, Esler M. The human sympathetic nervous system: its relevance in hypertension and heart failure. *Eur Heart J*. 2012;33:1058–1066.
- Ma X, Abboud FM, Chapleau MW. Analysis of afferent, central, and efferent components of the baroreceptor reflex in mice. *Am J Physiol Regul Integr Comp Physiol*. 2002;283:R1033–R1040.
- Liu C, Bookout AL, Lee S, Sun K, Jia L, Lee C, Udit S, Deng Y, Scherer PE, Mangelsdorf DJ, Gautron L, Elmquist JK. PPAR γ in vagal neurons regulates high-fat diet induced thermogenesis. *Cell Metab*. 2014;19:722–730.
- Lu Y, Ma X, Sabharwal R, Snitsarev V, Morgan D, Rahmouni K, Drummond HA, Whiteis CA, Costa V, Price M, Benson C, Welsh MJ, Chapleau MW, Abboud FM. The ion channel ASIC2 is required for baroreceptor and autonomic control of the circulation. *Neuron*. 2009;64:885–897.
- Sun H, Li DP, Chen SR, Hittelman WN, Pan HL. Sensing of blood pressure increase by transient receptor potential vanilloid 1 receptors on baroreceptors. *J Pharmacol Exp Ther*. 2009;331:851–859.
- Li L, Huang C, Ai J, Yan B, Gu H, Ma Z, Li AY, Xinyan S, Harden SW, Hatcher JT, Wurster RD, Cheng ZJ. Structural remodeling of vagal afferent innervation of aortic arch and nucleus ambiguus (NA) projections to cardiac ganglia in a transgenic mouse model of type 1 diabetes (OVE26). *J Comp Neurol*. 2010;518:2771–2793.
- Loo L, Shepherd AJ, Mickle AD, Lorca RA, Shutov LP, Usachev YM, Mohapatra DP. The C-type natriuretic peptide induces thermal hyperalgesia through a noncanonical G $\beta\gamma$ -dependent modulation of TRPV1 channel. *J Neurosci*. 2012;32:11942–11955.
- Kleinhenz JM, Kleinhenz DJ, You S, Ritzenthaler JD, Hansen JM, Archer DR, Sutliff RL, Hart CM. Disruption of endothelial peroxisome proliferator-activated receptor- γ reduces vascular nitric oxide production. *Am J Physiol Heart Circ Physiol*. 2009;297:H1647–H1654.
- Nicol CJ, Adachi M, Akiyama TE, Gonzalez FJ. PPAR γ in endothelial cells influences high fat diet-induced hypertension. *Am J Hypertens*. 2005;18(4 pt 1):549–556.

17. Beyer AM, de Lange WJ, Halabi CM, Modrick ML, Keen HL, Faraci FM, Sigmund CD. Endothelium-specific interference with peroxisome proliferator activated receptor gamma causes cerebral vascular dysfunction in response to a high-fat diet. *Circ Res*. 2008;103:654–661.
18. Subramanian V, Golledge J, Ijaz T, Bruemmer D, Daugherty A. Plioglitazone-induced reductions in atherosclerosis occur via smooth muscle cell-specific interaction with PPAR{gamma}. *Circ Res*. 2010;107:953–958.
19. Marchesi C, Rehman A, Rautureau Y, Kasal DA, Briet M, Leibowitz A, Simeone SM, Ebrahimiyan T, Neves MF, Offermanns S, Gonzalez FJ, Paradis P, Schiffrin EL. Protective role of vascular smooth muscle cell PPAR γ in angiotensin II-induced vascular disease. *Cardiovasc Res*. 2013;97:562–570.
20. Chapeau MW, Sabharwal R. Methods of assessing vagus nerve activity and reflexes. *Heart Fail Rev*. 2011;16:109–127.
21. Lohmeier TE, Iliescu R. Chronic activation of the baroreflex and the promise for hypertension therapy. *Handb Clin Neurol*. 2013;117:395–406.
22. Huber DA, Schreihof AM. Attenuated baroreflex control of sympathetic nerve activity in obese Zucker rats by central mechanisms. *J Physiol*. 2010;588(pt 9):1515–1525.
23. Nakamura Y, Takeda K, Nakata T, Hayashi J, Kawasaki S, Lee LC, Sasaki S, Nakagawa M, Ijichi H. Central attenuation of aortic baroreceptor reflex in prehypertensive DOCA-salt-loaded rats. *Hypertension*. 1988;12:259–266.
24. Gonzalez ER, Krieger AJ, Sapru HN. Central resetting of baroreflex in the spontaneously hypertensive rat. *Hypertension*. 1983;5:346–352.
25. Chapeau MW, Cunningham JT, Sullivan MJ, Wachtel RE, Abboud FM. Structural versus functional modulation of the arterial baroreflex. *Hypertension*. 1995;26:341–347.
26. Pelat M, Dessy C, Massion P, Desager JP, Feron O, Balligand JL. Rosuvastatin decreases caveolin-1 and improves nitric oxide-dependent heart rate and blood pressure variability in apolipoprotein E-/- mice in vivo. *Circulation*. 2003;107:2480–2486.
27. Sapru HN, Wang SC. Modification of aortic baroreceptor resetting in the spontaneously hypertensive rat. *Am J Physiol*. 1976;230:664–674.
28. Pelham CJ, Keen HL, Lentz SR, Sigmund CD. Dominant negative PPAR γ promotes atherosclerosis, vascular dysfunction, and hypertension through distinct effects in endothelium and vascular muscle. *Am J Physiol Regul Integr Comp Physiol*. 2013;304:R690–R701.
29. Gollasch M, Tank J, Luft FC, Jordan J, Maass P, Krasko C, Sharma AM, Busjahn A, Bähring S. The BK channel beta1 subunit gene is associated with human baroreflex and blood pressure regulation. *J Hypertens*. 2002;20:927–933.
30. Bernardo A, Ajmone-Cat MA, Gasparini L, Ongini E, Minghetti L. Nuclear receptor peroxisome proliferator-activated receptor-gamma is activated in rat microglial cells by the anti-inflammatory drug HCT1026, a derivative of flurbiprofen. *J Neurochem*. 2005;92:895–903.
31. Cimini A, Benedetti E, Cristiano L, Sebastiani P, D'Amico MA, D'Angelo B, Di Loreto S. Expression of peroxisome proliferator-activated receptors (PPARs) and retinoic acid receptors (RXRs) in rat cortical neurons. *Neuroscience*. 2005;130:325–337.
32. Lu M, Sarruf DA, Talukdar S, Sharma S, Li P, Bandyopadhyay G, Nalbandian S, Fan W, Gayen JR, Mahata SK, Webster NJ, Schwartz MW, Olefsky JM. Brain PPAR- γ promotes obesity and is required for the insulin-sensitizing effect of thiazolidinediones. *Nat Med*. 2011;17:618–622.
33. Ryan KK, Li B, Grayson BE, Matter EK, Woods SC, Seeley RJ. A role for central nervous system PPAR- γ in the regulation of energy balance. *Nat Med*. 2011;17:623–626.
34. Caterina MJ, Schumacher MA, Tominaga M, Rosen TA, Levine JD, Julius D. The capsaicin receptor: a heat-activated ion channel in the pain pathway. *Nature*. 1997;389:816–824.
35. Basbaum AI, Bautista DM, Scherrer G, Julius D. Cellular and molecular mechanisms of pain. *Cell*. 2009;139:267–284.
36. Wu JS, Lu FH, Yang YC, Chang SH, Huang YH, Chen JJ, Chang CJ. Impaired baroreflex sensitivity in subjects with impaired glucose tolerance, but not isolated impaired fasting glucose [published online ahead of print January 2014]. *Acta Diabetol*. doi: 10.1007/s00592-013-0548-9. <http://link.springer.com/article/10.1007%2Fs00592-013-0548-9>. Accessed June 2, 2014.
37. Frattola A, Parati G, Gamba P, Paleari F, Mauri G, Di Rienzo M, Castiglioni P, Mancia G. Time and frequency domain estimates of spontaneous baroreflex sensitivity provide early detection of autonomic dysfunction in diabetes mellitus. *Diabetologia*. 1997;40:1470–1475.
38. Maeda CY, Fernandes TG, Timm HB, Irigoyen MC. Autonomic dysfunction in short-term experimental diabetes. *Hypertension*. 1995;26(6 pt 2):1100–1104.
39. Lin M, Harden SW, Li L, Wurster RD, Cheng ZJ. Impairment of baroreflex control of heart rate in conscious transgenic mice of type 1 diabetes (OVE26). *Auton Neurosci*. 2010;152:67–74.
40. Okada N, Takahashi N, Yufu K, Murozono Y, Wakisaka O, Shinohara T, Anan F, Nakagawa M, Hara M, Saikawa T, Yoshimatsu H. Baroreflex sensitivity predicts cardiovascular events in patients with type 2 diabetes mellitus without structural heart disease. *Circ J*. 2010;74:1379–1383.
41. Yokoe H, Yuasa F, Yuyama R, Murakawa K, Miyasaka Y, Yoshida S, Tsujimoto S, Sugiura T, Iwasaka T. Effect of pioglitazone on arterial baroreflex sensitivity and sympathetic nerve activity in patients with acute myocardial infarction and type 2 diabetes mellitus. *J Cardiovasc Pharmacol*. 2012;59:563–569.
42. Zhao D, McCully BH, Brooks VL. Rosiglitazone improves insulin sensitivity and baroreflex gain in rats with diet-induced obesity. *J Pharmacol Exp Ther*. 2012;343:206–213.

Novelty and Significance

What Is New?

- Mice expressing dominant-negative proliferator-activated receptor- γ specifically in vascular smooth muscle (S-P467L) exhibit increased sympathetic activity to the heart and decreased effectiveness of the baroreflex.
- S-P467L mice exhibit decreased aortic depressor nerve activity in response to changes in arterial pressure, whereas arterial pressure and heart rate responses to direct aortic depressor nerve stimulation were similar in S-P467L and control mice
- These data suggest that the afferent limb of the baroreflex arc is impaired, whereas the central and efferent limbs of the baroreflex arc remain intact.

What Is Relevant?

- Proliferator-activated receptor- γ is a ligand-activated transcription factor classically playing an important role in adipogenesis and metabolic processes but more recently cardiovascular diseases such as hypertension.

- The baroreflex is an important beat-to-beat regulator of arterial pressure and heart rate, controlled by baroreceptors, located in the adventitia of the aortic arch and carotid sinus.

Summary

The most important observations from this study relate to the finding that mice with impaired proliferator-activated receptor- γ activity in vascular smooth muscle exhibit tachycardia mechanistically caused by any combination of (1) increased cardiac sympathetic nervous system activity, (2) impaired baroreflex regulation, and (3) a blunted aortic depressor nerve response to increased arterial pressure localized to the afferent limb of the baroreflex arc. Therefore, there may be some degree of baroreflex failure in S-P467L mice, which drives the increased heart rate. These findings implicate vascular smooth muscle proliferator-activated receptor- γ as a critical determinant of neurovascular signaling.

Interference With Peroxisome Proliferator-Activated Receptor- γ in Vascular Smooth Muscle Causes Baroreflex Impairment and Autonomic Dysfunction

Giulianna R. Borges, Donald A. Morgan, Pimonrat Ketsawatsomkron, Aaron D. Mickle, Anthony P. Thompson, Martin D. Cassell, Durga P. Mohapatra, Kamal Rahmouni and Curt D. Sigmund

Hypertension. 2014;64:590-596; originally published online June 9, 2014;

doi: 10.1161/HYPERTENSIONAHA.114.03553

Hypertension is published by the American Heart Association, 7272 Greenville Avenue, Dallas, TX 75231

Copyright © 2014 American Heart Association, Inc. All rights reserved.

Print ISSN: 0194-911X. Online ISSN: 1524-4563

The online version of this article, along with updated information and services, is located on the World Wide Web at:

<http://hyper.ahajournals.org/content/64/3/590>

Data Supplement (unedited) at:

<http://hyper.ahajournals.org/content/suppl/2014/06/09/HYPERTENSIONAHA.114.03553.DC1.html>

Permissions: Requests for permissions to reproduce figures, tables, or portions of articles originally published in *Hypertension* can be obtained via RightsLink, a service of the Copyright Clearance Center, not the Editorial Office. Once the online version of the published article for which permission is being requested is located, click Request Permissions in the middle column of the Web page under Services. Further information about this process is available in the [Permissions and Rights Question and Answer](#) document.

Reprints: Information about reprints can be found online at:

<http://www.lww.com/reprints>

Subscriptions: Information about subscribing to *Hypertension* is online at:

<http://hyper.ahajournals.org/subscriptions/>

Supplemental Materials

Interference with PPAR γ in Vascular Smooth Muscle Causes Baroreflex Impairment and Autonomic Dysfunction

Giulianna R. Borges¹, Donald A. Morgan¹, Pimonrat Ketsawatsomkron¹, Aaron D. Mickle¹, Anthony P. Thompson², Martin D. Cassell², Durga P. Mohapatra¹, Kamal Rahmouni^{1,3}, and Curt D. Sigmund^{1,3}

Supplemental Methods

Mice. Male transgenic mice (6 months of age) expressing the dominant negative PPAR γ P467L mutation under the control of the smooth muscle myosin heavy chain promoter (S-P467L) were used¹. Age-matched male non-transgenic (NT) littermates were utilized as controls. Mice were housed in a room with controlled temperature (23°C) and dark/light cycle of 12 hours. All mice had free access to water and standard rodent chow. All procedures were approved by Institutional Animal Care and Use Committee.

Baseline Cardiovascular Evaluation. Radiotelemetry devices (Data Sciences International) were used to record arterial pressure and heart rate. Under ketamine-xylazine anesthesia (85.5 mg/kg:12.5 mg/kg), radiotelemeter catheters implanted into the left common carotid artery through an anterior neck incision. The radiotelemeter transmitter was implanted subcutaneously into the right flank. After 10 days of recovery, basal direct arterial pressure and heart rate were recorded for one hour. The sympathetic or the vagal effects to the heart were assessed by autonomic blockade with propranolol (5 mg/kg, i.p.) or methyl-atropine (2 mg/kg, i.p.), respectively. The intrinsic heart rate, the heart rate without any influence of the autonomic nervous system, was calculated after simultaneous β -adrenergic and muscarinic blockade. On the following day, the protocol was repeated inverting the sequence of the autonomic blockers. All experiments were sampled in a high frequency (2000 Hz) and performed between 9 AM and 12 PM. The spontaneous activity of the baroreflex was determined from the arterial pressure basal recording using the sequence method as previously described.^{2,3} Data from the basal recording were utilized to determine the low (LF) and high frequency (HF) components of the arterial pressure and heart rate variability by using the spectral analysis.⁴

Baroreflex Regulation of Heart Rate in Conscious Mice. Mice were anesthetized with Isoflurane (2% concentration level) and the right jugular vein and left carotid artery were cannulated with microrenathane tubing. The venous and arterial cannula were tunneled subcutaneously around the opposite forelimb and then exited out of the nape of the neck. The arterial cannula was connected to a pressure transducer (BP-100, ADInstruments) for continuous monitoring of blood pressure throughout the experiment. Each mouse was allowed 2-3 hours to fully recover from the effects of the surgery and the influence of isoflurane anesthesia in order to establish a stable baseline blood pressure and heart rate in the conscious state. A slow infusion of PE (5 μ g, 5 μ l volume) was given followed by a 25 μ l iv saline flush. When baseline blood pressure and heart rate were re-established, SNP (5 μ g, 5 μ l volume) was slowly given through the venous cannula followed by a 25 μ l iv saline flush. This dose of PE and SNP (5 μ g) was found to elicit near-maximal responses in the increase and decrease in blood pressure in the conscious mouse without any adverse effects. At the end of the experiment, mice were killed with anesthetic overdose.

Assessment of aortic depressor nerve (ADN) activity. Mice were anesthetized with ketamine-xylazine (85.5 mg/kg:12.5 mg/kg) and the left femoral artery and right jugular vein were cannulated with microrenathane tubing to allow direct arterial pressure recording and drug infusion, respectively. By means of an anterior neck incision, left aortic depressor nerve (ADN) was carefully isolated using a dissecting microscope. The ADN was placed on a bipolar platinum electrode and encased with silicone gel (Kwik-Cast; WPI). The nerve activity was amplified and filtered and its unique activity was identified as synchronized bursts with the beginning of systolic cycle as described previously.⁵ The anesthesia was sustained with intravenous administration of α -chloralose (25mg/kg/h, i.v.). Baseline ADN activity and hemodynamic parameters were recorded for 10 -15 minutes and then the afferent component of the baroreflex was challenged by slow infusion (20 μ L/min) of sodium nitroprusside (SNP; 1-

5 μ g/g) immediately followed by phenylephrine (PE; 4-20 μ g/g). After all parameters returned to baseline conditions, the ADN was crushed at a point caudal to the electrode (to avoid any arterial pressure-induced responses) to evaluate the central component of the baroreflex. The same electrode used to perform the recording was connected to a stimulator (Grass, SIU 5) and the ADN was stimulated with a rectangular 10V, 2ms duration pulses that were delivered in random frequencies (2, 5, 15, 30 and 40Hz) over 10s. At the end of the experiment, mice were killed with anesthetic overdose.

Data Analysis.

1. Baseline Arterial Pressure and Heart Rate: Radiotelemetry arterial pressure recordings were analyzed by a computer software designed to detect inflection points of a periodic wave (Advanced CODAS, Dataq Instruments, OH, USA). Beat-by-beat time series of systolic, diastolic and mean arterial pressure were generated and heart rate was measured from successive diastolic pulse intervals.

2. Cardiac Autonomic Indexes and Intrinsic Heart Rate: Cardiac sympathetic and vagal effects were assessed by autonomic blockade produced by injection of propranolol and methyl atropine, respectively. The difference between the heart rate after propranolol administration and basal heart rate was considered as the sympathetic effect to the heart. Similarly, the difference between the heart rate after methyl atropine administration and basal heart rate was considered as the vagal effect to the heart. The heart rate calculated when both autonomic blockers were simultaneously administered was considered as the intrinsic heart rate.

3. Spontaneous Baroreflex Sensitivity (SBRS): The baseline baroreflex control of heart rate was assessed through spontaneous changes in arterial pressure and pulse interval by the sequence method described by Bertinieri and coworkers.³ Ramps of progressive increases and decreases in systolic arterial pressure were automatically detected in 104 beats pulsatile arterial pressure recordings using the freely available HemoLab computer software (<http://www.intergate.com/~harald/HemoLab/Hemolab.html>). Sequences defined ramps of four or more systolic arterial pressure values associated with parallel changes in pulse interval (i.e. systolic arterial pressure increases and pulse interval lengthening as well as systolic arterial pressure decreases and pulse interval shortenings). The SBRS was calculated from the slope (ms/mmHg) of linear regression lines between the systolic arterial pressure and the subsequent pulse interval. Only regression lines with a correlation coefficient higher than 0.85 were considered. The average of the slopes of all individual regression lines was then used as an index of BRS. The baroreflex effectiveness index (BEI), which provides information on the baroreflex function that is complementary to BRS was also calculated. It is defined as the ratio between the number of systolic arterial pressure ramps followed by the respective reflex changes in pulse interval, and the total number of systolic arterial pressure ramps (independently on whether they are or not accompanied by the corresponding reflex pulse interval ramps) observed over the time window studied.

4. Spectral Analysis: From the baseline recordings, the time series of systolic arterial pressure and pulse interval were divided into contiguous segments of 350 beats, overlapped by one-half. Mean and variance of each segment were calculated and submitted to a model-based autoregressive spectral analysis. The power of the oscillatory components was quantified in two frequency bands: low frequency (LF; 0.1–1 Hz) and high frequency (HF; 1–5 Hz). Oscillations slower than 0.1 Hz were not quantified in this study.

5. Afferent and Central Components of Baroreflex Function: The baroreflex function and ADN stimulation were analyzed as described previously.⁵ Levels of ADN activity were normalized as

a percentage of the maximum level of activity recorded during PE and SNP administration, respectively. The relationship between mean arterial pressure (MAP) and nerve activity was determined by fitting the data to a sigmoidal logistic function. The logistic function for control of ADN conformed to the mathematical expression $Y = P1 / \{1 + \exp[P2 (X - P3)]\} + P4$, where $X = \text{MAP}$, $Y = \text{ADNA (\%max)}$, $P1 = \text{maximum} - \text{minimum ADNA (range)}$, $P2 = \text{slope coefficient}$, $P3 = \text{MAP at 50\% of ADNA range}$, and $P4 = \text{maximum ADNA}$. $P1$ (ADNA range) was expressed as a negative value. The maximum slope (gain) was calculated as $P1 = P2/4$. The MAP threshold (MAP_{th}) and saturation (MAP_{sat}) pressures were calculated from the third derivative of the logistic function. The central component of the baroreflex loop was evaluated by the difference between the peak changes in systolic arterial pressure and heart rate and their baseline values measured in response to graded electrical stimulation (2, 5, 15, 30 and 40Hz) of the ADN.

Mechanical Properties of Carotid Artery. Left carotid arteries from NT and S-P467L mice were isolated and mounted into a pressurized myograph system (Danish Myo Technology). Intraluminal pressure was increased slowly from 5 mmHg to 75 mmHg and the vessel was equilibrated for 30 min in Ca^{2+} free Krebs buffer containing 10⁻⁵ M SNP and 2 mM EGTA. Carotid arteries were then subjected to a series of pressure from 10 mmHg to 150 mmHg and from 150 mmHg to 5 mmHg (back and forth) twice to remove hysteresis. The sequence of pressure was done as follows: P 0, 10, 20, 30, 40, 50, 75, 100, 125 and 150 mmHg. Lastly, internal and external diameter were recorded after subjecting the vessel to pressures of P0, 10, 20, 30, 50, 75, 100, 125 and 150 mmHg. In some studies, vessels were exposed to pressure of 25, 50, 75, 100, 125 and 150 mmHg. The distensibility was calculated by normalized compliance with the luminal cross sectional area. Luminal cross-sectional area and cross-sectional compliance were calculated as described previously.⁶ Stress-strain curve and its slope were calculated as previously described.⁷

Quantitative real-time RT-PCR (qRT-PCR). Nodose ganglia and aorta were isolated from S-P467L and littermate controls. Four ganglia obtained from two mice were pooled for each sample. Tissues were snap frozen in liquid nitrogen and RNA was extracted using Trizol (Invitrogen). Total RNA was isolated using a silica spin column (Purelink RNA mini kit, Invitrogen) following the manufacturer's protocol. The RNA concentration was determined by using a NanoDrop ND-1000 and cDNA was generated by RT-PCR using SuperScript III (Invitrogen). qRT-PCR was performed using the TaqMan (Applied Biosystems) gene expression assay according to company's instruction. The assay numbers for TaqMan (Applied Biosystems) were the following: Mm00475691_m1 (mouse Asic2), Mm00805460_m1 (mouse Asic3), Mm01246283_m1 (mouse Trpv1), and Mm99999915_g1 (mouse GAPDH). The Taqman probe that specifically detected human PPAR γ was custom made and designed to anneal in sequences that differ between mouse and human PPAR γ .

Neurovascular Coupling: To determine if there were any differences in the fiber composition of the ADN nerve plexuses in the aortic arch we immunochemically stained whole mount preparations with an antibody to transient receptor potential vanilloid 1 receptors (Trpv1). Trpv1 has been identified in both small/medium myelinated (A δ) and small unmyelinated fibers in the ADN and depletion and blockade of Trpv1 decrease the maximum gain of the baroreflex.⁸ Five NT and S-P467L mice were perfused under anesthesia through the left ventricle with 100ml of 4% paraformaldehyde and 0.1% glutaraldehyde in 0.1M PBS. The thoracic contents were removed en bloc and post-fixed in the perfusing solution overnight. The aortic arch and most of the surrounding adipose tissue were dissected out and placed in PBS containing 0.5% Triton-X. Arch specimens were then placed in blocking serum for 1 hour followed by 48 hour incubation in a rabbit anti-Trpv1 antibody (NeuroMics) diluted 1:1000 in PBS with 0.5% Triton-X. After

washing, whole arches were incubated for 2 hours in a biotinylated goat anti-rabbit antibody (1:200 dilution) followed by 1 hour in avidin-HRP. Peroxidase activity was detected using 3,3'-diaminobenzidine. Specimens were then washed in PBS, dehydrated in ethanol and cleared in Citrosol and xylene before being mounted in well slides with Permount. To determine any differences in fiber composition, low power (10X) images were taken from three areas in each aortic arch in the vicinity of the origin of the left common carotid and subclavian arteries, viz. the major termination area of the left ADN. Using Adobe Photoshop, a 250 μ m X 250 μ m grid divided into 25 50 μ m X 50 μ m squares was digitally placed over each image and the numbers of grid line intersections with thick (presumed myelinated) and fine (presumed unmyelinated) fibers were counted. Counts were pooled for aortic arches from each animal group and compared using a t-test.

Primary cultures of mouse nodose ganglia (NG) neurons: NGs were isolated from adult S-P467L and NT mice, and cultured on glass coverslips, as described previously for mouse dorsal root ganglia (DRG) neurons.⁹ Briefly, isolated NGs were digested with collagenase for 20 min at 37°C, followed by centrifugation and resuspension with Dulbecco's modified Eagle's Medium (DMEM; Life Technologies, Green Islands, NY) supplemented with 10% fetal bovine serum (FBS), and subsequently digested with pronase for 10 min at 37°C. Cells were then pelleted by centrifugation and re-suspended in DMEM + 10% FBS, before further trituration with fire-polished glass Pasteur pipettes. Cells were then plated onto poly-L-ornithine- and laminin-coated glass coverslips. Following 2 h incubation at 37°C in a 5% CO₂ incubator, the culture media was changed to TNB media supplemented with protein-lipid complex (Biochrom AG, Berlin, Germany), and cultured for 2 days *in vitro* (DIV) at 37°C in a 5% CO₂ incubator.

Calcium imaging: Functional Ca²⁺ imaging on cultured mouse NG neurons (2 DIV) was performed to assess the magnitude and characteristics of TRPV1 activity, as described previously in DRG neurons.⁹ Neurons on glass coverslips were incubated under dark condition at room temperature (22°C) for 30 min with 2 μ M of the AM form of the Ca²⁺-sensitive dye Fura-2 (Life Technologies). The coverslip was then placed in the recording chamber mounted on the stage of an inverted IX-71 microscope (Olympus Co., Tokyo, Japan) and washed for 10 min before the experiment began. Fluorescence was alternately excited at 340 nm and 380 nm (both 12 nm band pass) using the Polychrome IV monochromator (T.I.L.L. Photonics, Martinsried, Germany), via a 10X objective [numerical aperture (NA) 0.75; Olympus]. Emitted fluorescence was collected at 510 (80) nm using an IMAGO CCD camera (T.I.L.L. Photonics). Pairs of 340/380 nm images were sampled at 0.2 Hz. The recording chamber was bathed with extracellular buffer containing (in mM) 115 NaCl, 5 KCl, 1.3 CaCl₂, 0.5 MgCl₂, 0.4 MgSO₄, 0.4 KH₂PO₄, 0.6 Na₂HPO₄, 0.5 NaHCO₃, 10 HEPES, 10 D-glucose, pH adjusted to 7.4, and osmolarity adjusted to 310 Osm. Bath application of capsaicin (100 nM, 15 sec) was performed twice with a 5 min interval. After the 2nd capsaicin application cells were washed with extracellular buffer for 4 min, followed by the application of KCl (50 mM, 30 sec). The fluorescence data were processed and analyzed using TILLvisION 4.0.1.2 (T.I.L.L. Photonics) and Prism-6 (Graphpad Software Inc., La Jolla, CA) software, and presented as fluorescence ratio ($R = F_{340}/F_{380}$), wherein an increase in the F_{340}/F_{380} ratio directly indicates an increase in intracellular Ca²⁺ ([Ca²⁺]_i) levels. In order to compare the maximal capsaicin response of NG neurons from both genotypes, the peak of 1st capsaicin-induced increase in [Ca²⁺]_i was normalized to the peak of KCl-induced increase in [Ca²⁺]_i in the same neuron. For quantification of the magnitude of TRPV1 channel desensitization, the ratio of 2nd vs 1st capsaicin-induced peak [Ca²⁺]_i in the same neuron was calculated, and presented as mean \pm SEM of F_{340}/F_{380} . All the Ca²⁺ imaging experiments were performed in triplicate across three different batches of mouse NG neuron cultures from both genotypes, simultaneously.

Statistical Analysis. All data are expressed as mean \pm SEM. Comparison between S-P467L and NT mice were made using student *t*-test. When normality failed, the data was analyzed with the Mann-Whitney Rank Sum Test. The baroreflex sigmoidal curves were compared using two-way ANOVA with repeated measures. The effects of stimulation on arterial pressure and heart rate were compared using ANOVA followed by Tukey's post hoc test. The level of significance considered in the present study was $p < 0.05$.

Supplemental References

1. Halabi CM, Sigmund CD. Peroxisome proliferator-activated receptor-gamma and its agonists in hypertension and atherosclerosis : mechanisms and clinical implications. *Am J Cardiovasc Drugs*. 2005;5:389-398.
2. Borges GR, Salgado HC, Silva CA, Rossi MA, Prado CM, Fazan R, Jr. Changes in hemodynamic and neurohumoral control cause cardiac damage in one-kidney, one-clip hypertensive mice. *Am J Physiol Regul Integr Comp Physiol*. 2008;295:R1904-R1913.
3. Bertinieri G, di RM, Cavallazzi A, Ferrari AU, Pedotti A, Mancia G. A new approach to analysis of the arterial baroreflex. *J Hypertens Suppl*. 1985;3:S79-S81.
4. Fazan R, Jr., de OM, da Silva VJ, Joaquim LF, Montano N, Porta A, Chappleau MW, Salgado HC. Frequency-dependent baroreflex modulation of blood pressure and heart rate variability in conscious mice. *Am J Physiol Heart Circ Physiol*. 2005;289:H1968-H1975.
5. Ma X, Abboud FM, Chappleau MW. Analysis of afferent, central, and efferent components of the baroreceptor reflex in mice. *Am J Physiol Regul Integr Comp Physiol*. 2002;283:R1033-R1040.
6. Belin de Chantemele EJ, Retailleau K, Pinaud F, Vessieres E, Bocquet A, Guihot AL, Lemaire B, Domenga V, Baufreton C, Loufrani L, Joutel A, Henrion D. Notch3 is a major regulator of vascular tone in cerebral and tail resistance arteries. *Arterioscler Thromb Vasc Biol*. 2008;28:2216-2224.
7. Baumbach GL, Sigmund CD, Bottiglieri T, Lentz SR. Structure of cerebral arterioles in cystathionine beta-synthase-deficient mice. *Circ Res*. 2002;91:931-937.
8. Sun H, Li DP, Chen SR, Hittelman WN, Pan HL. Sensing of blood pressure increase by transient receptor potential vanilloid 1 receptors on baroreceptors. *J Pharmacol Exp Ther*. 2009;331:851-859.
9. Loo L, Shepherd AJ, Mickle AD, Lorca RA, Shutov LP, Usachev YM, Mohapatra DP. The C-type natriuretic peptide induces thermal hyperalgesia through a noncanonical Gbetagamma-dependent modulation of TRPV1 channel. *J Neurosci*. 2012;32:11942-11955.

Supplemental Figures

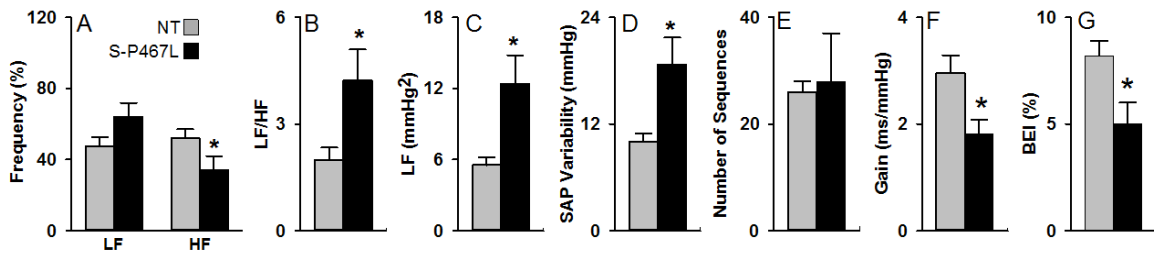


Figure S1. *Spectral Analysis and Spontaneous Baroreflex Function.*

Power spectral analysis of heart rate and arterial pressure variability is shown. A) Relative low frequency (LF) and high frequency (HF) components of heart rate variability. B) LF/HF ratio of HR variability. C) Magnitude of the LF component of AP variability. D) Systolic arterial pressure (SAP) variability. E) Number of baroreflex sequences. F) Gain of spontaneous baroreflex. G) Baroreflex effectiveness index. S-P467L (black) and non-transgenic (gray) mice. N=8 per group; *, P<0.05 vs NT.;**, P<0.05 HF vs LF.

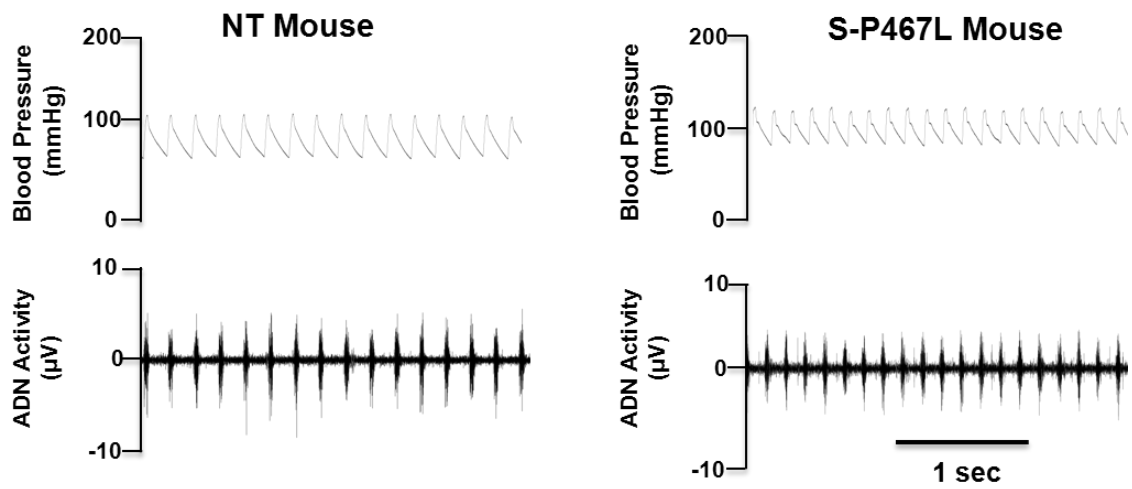


Figure S2: *ADN Activity*. Representative tracings showing coupling between blood pressure and ADN firing.

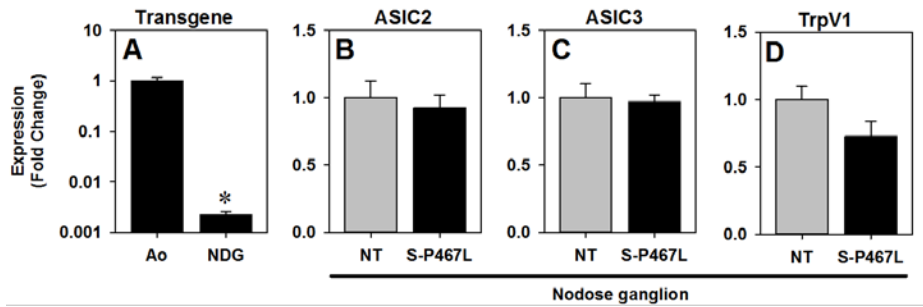


Figure S3: *Gene expression in nodose ganglion.* A) Gene expression of hPPAR γ in S-P467L nodose ganglion (NG) compared to those in aorta (Ao) are shown. B-D) mRNA expression of Asic2 (B), Asic3 (C) and Trpv1 (D) in NG comparing NT with S-P467L. N=4 for S-P467L; N=3 for NT; *, P<0.05 vs NT.